A Molecular Dynamics Study of the Atomic Structure of $(CaO)_x(SiO_2)_{1-x}$ Glasses

Robert N. Mead and Gavin Mountjoy*

School of Physical Sciences, University of Kent, Canterbury CT2 7NH, United Kingdom

Received: May 11, 2006

The local atomic environment of Ca in $(CaO)_x(SiO_2)_{1-x}$ glasses is of interest because of the role of Ca in soda-lime glass, the application of calcium silicate glasses as biomaterials, and the previous experimental measurement of the Ca−Ca correlation in $CaSiO_3$ glass. Molecular dynamics has been used to obtain models of $(CaO)_x(SiO_2)_{1-x}$ glasses with $x = 0$, 0.1, 0.2, 0.3, 0.4, and 0.5, and with ∼1000 atoms and size ∼25 Å. As expected, the models contain a tetrahedral silica network, the connectivity of which decreases as x increases. In the glass-forming region, i.e., $x = 0.4$ and 0.5, Ca has a mixture of 6- and 7-fold coordination. Bridging oxygen makes an important contribution to the coordination of Ca, with most bridging oxygens coordinated to 2 Si plus 1 Ca. The $x = 0.5$ model is in reasonable agreement with previous experimental studies, and does not substantiate the previous theory of cation ordering, which predicted Ca arranged in sheets. In the phase-separated region, i.e., $x = 0.1$ and 0.2, there is marked clustering of Ca.

1. Introduction

Studying the atomic structure of calcium silicate glasses, $(CaO)_x(SiO_2)_{1-x}$, is worthwhile for several reasons. The most common form of glass is soda-lime glass, $(Na_2O)_y(CaO)_x(SiO_2)_{1-x-y}$, and Ca makes an essential contribution to the versatility of this glass, which is optimized for $x \approx 0.10$ and $y \approx 0.15$.[1] Information about the local atomic environment of Ca in $(CaO)_x(SiO_2)_{1-x}$ glasses should assist in understanding the role of Ca in soda-lime silicate and other ternary systems. $CaSiO_3$ glass ($x = 0.50$) is one of the very few glasses for which the cation−cation distribution, i.e., Ca−Ca correlation, has been experimentally measured.[2] Hence it provides a benchmark for theories of modifier cation ordering in silicate glasses. The previous measurements were interpreted as showing cation ordering similar to that in crystalline $CaSiO_3$ wollastonite, which has Ca arranged in sheets.[2] In addition, amorphous calcium silicate $(CaO)_x(SiO_2)_{1-x}$ sol−gels are bioactive materials.[3] The bioactivity is found to vary with composition and to be enhanced for $x \approx 0.3$.[3]

The $CaO-SiO_2$ system is immiscible for $0 < x < 0.3$, where there is a 2 liquid region with liquidus temperature of 1978 K and critical temperature of 2144 K.[4] In the glass-forming region, the liquidus has a minimum of 1709 K at $x \approx 0.4$, rising to 1817 K at $x = 0.5$. There have been several structural studies of $CaSiO_3$ glass ($x = 0.5$). The data include density,[5] X-ray diffraction,[6,7] Ca K-edge EXAFS,[7,8] ^{17}O and ^{29}Si NMR,[9,10] and neutron diffraction with isotopic substitution.[2] The results are consistent with a tetrahedral silica network, and with Ca acting as a network modifier, with Ca−O coordination of ∼6. Neutron diffraction with double difference isotopic substitution was used to measure the Ca−Ca correlation,[2] one of the very few times this has been done for a glass. The results were interpreted as being similar to those in crystalline $CaSiO_3$ wollastonite,[11] implying similar cation ordering, with sheets of octahedrally coordinated Ca. X-ray[12] and neutron diffraction[13] structure factors have also been reported for glasses with $x = 0.42$.

The measurement of the Ca−Ca distribution for $x = 0.5$ glass prompted a single previous computer modeling study of $(CaO)_x(SiO_2)_{1-x}$ glasses using molecular dynamics.[14] However, for $x = 0.5$ that study reported an unrealistic Si−O distance of 1.7 Å and Si−O coordination of 4.7, so there is scope for improved models of the atomic structure. This paper presents a new molecular dynamics study of the structure of $(CaO)_x(SiO_2)_{1-x}$ glasses. Compositions of $x = 0$, 0.1, 0.2, 0.3, 0.4, and 0.5 have been modeled. This range includes pure SiO_2 ($x = 0$) as a reference structure, the phase-separated region ($x = 0.1$ and 0.2), and the glass-forming region ($x = 0.4$ and 0.5), the latter being the main focus of interest.

2. Molecular Dynamics Method

Interatomic potentials for $(CaO)_x(SiO_2)_{1-x}$ were obtained from the literature. Five different potentials were evaluated.[14−18] All of these used 2-body terms of the form:

$$V_{ij}(r) = \frac{q_i q_j}{4\pi\epsilon_0 r_{ij}} + A_{ij}\exp\left(\frac{-r_{ij}}{\rho}\right) - \frac{C_{ij}}{r_{ij}^{\,6}} \qquad (1)$$

where $V_{ij}(r)$ is the potential, i and j are elements, r is distance, q is charge, and A, ρ, and C are potential parameters (and $\epsilon_0 = 8.854 \times 10^{-12}\ C^2\ N^{-1}\ m^{-2}$). (One of the potentials also included a 3-body term for O−Si−O interactions.[17]) The different potentials were evaluated by using the GULP program[19] to model crystalline $(CaO)_x(SiO_2)_{1-x}$ compounds: lime (CaO),[20] α-quartz (SiO_2),[21] olivine (Ca_2SiO_4),[22] wollastonite ($CaSiO_3$),[11] and pseudowollastonite ($CaSiO_3$)[23] (the data were obtained from CDS, UK[24]). The potential from Cormack and Du[15] was judged to be the most suitable, as overall it reproduced best the nearest neighbor distances for Si and Ca, bond angles for Si, and values of bulk modulus, B.[18,23] The potential parameters are shown in Table 1, and the comparison between experimental and modeled crystal structures is shown in Table 2.

Molecular dynamics was used to obtain models of atomic structure of $(CaO)_x(SiO_2)_{1-x}$ glasses with compositions $x = 0$, 0.1, 0.2, 0.3, 0.4, and 0.5. Table 3 shows details of the models. Each model has ∼1000 atoms, in a cubic box with length ∼25 Å. Random starting configurations and periodic boundary

* Address correspondence to this author. E-mail: g.mountjoy@kent.ac.uk.

10.1021/jp0628939 CCC: $33.50
Published on Web 07/06/2006

TABLE 1: Potential Parameters Used in This Study[15]

$i-j$	q_i (e)	A_{ij} (eV)	ρ_{ij} (Å)	C_{ij} (eV Å^{-6})
Si−O	2.4	18003	0.205	133.5
Ca−O	1.2	131400	0.188	60.0
O−O	−1.2	1388	0.362	175
Ca−Ca	1.2	10000	0.230	0

TABLE 2: Comparison of Crystal Structures (see text for references) from Experiment (plain text) and Modeling (italic text)

structural parameter	CaO lime	SiO_2 α-quartz	Ca_2SiO_4 olivine	$CaSiO_3$ wollastonite	$CaSiO_3$ pseudo-wollastonite
a (Å)	4.81	4.91	5.08	7.93	6.86
	4.85	*4.94*	*5.23*	*7.92*	*6.84*
b (Å)	4.81	4.91	11.23	7.32	11.87
	4.85	*4.94*	*11.27*	*7.35*	*11.88*
c (Å)	4.81	5.41	6.76	7.07	19.63
	4.85	*5.45*	*6.78*	*7.19*	*20.10*
R_{SiO} (Å)		1.61	1.65	1.62	1.62
		1.60	*1.60*	*1.60*	*1.60*
R_{CaO} (Å)	2.40		2.37	2.40	2.47
	2.42		*2.43*	*2.47*	*2.46*
O−Si−O (deg)		109	109	109	109
		109	*109*	*109*	*109*
Si−O−Si (deg)		144		144	134
		148		*150*	*138*
B (Gpa)	111	38		100	86
	149	*40*	*114*	*115*	*95*

TABLE 3: Parameters of $(CaO)_x(SiO_2)_{1-x}$ Glass Models

x	density (g cm^{-3})	atoms	length (Å)
0.5	2.90	1000	23.70
0.4	2.78	1040	24.09
0.3	2.63	1080	24.59
0.2	2.47	1120	25.17
0.1	2.33	1160	25.72
0	2.19	1200	26.32

conditions were used. The modeling used the DLPOLY program,[25] with time steps of 2 fs, and with a Berensden NVT algorithm, with relaxation time of 2 ps. An NVT algorithm was used to obtain final densities compatible with the measured densities,[5] since this is one of the requirements to model the experimental glasses. All the non-Coulombic parts of the pair potentials (and only those) were subjected to a short-range cutoff of 10 Å. The Coulomb potential was calculated by using the Ewald sum method with a precision of 10^{-5}.

The modeling used a series of stages. The first 3 stages were temperature baths (with equilibration) at 6000, 3000, and 2000 K (and with linear thermal expansion of 1.03, 1.015, and 1.005 respectively) of 80 000 time steps each, corresponding to a simulation time of 160 ps. The liquid relaxation time τ can be estimated from the ratio of viscosity η to shear modulus G. Typical values of G are 3×10^{10} Pa for SiO_2,[26] and 10^{10} Pa for $Na_2Si_2O_5$.[27] Reported values of η at 2000 K are 10^6 Pa·s for SiO_2,[28] 10^0 Pa·s for soda-lime silicate[28] (approximately $x \sim 0.25$), and 10^{-1} Pa·s for $CaSiO_3$[29] ($x = 0.5$). This gives estimated values of τ at 2000 K of 30 μs for $x = 0$,[26] 100 ps for $x \sim 0.25$,[27] and 10 ps for $x = 0.5$, and the latter two values are less than the simulation times of 160 ps.

The fourth stage was a temperature quench of 60 000 time steps from 2000 to 300 K. The quench rate during modeling was 10^{13} K s^{-1}, which is typical for MD studies of glasses.[15−17,30] Due to constraints on computing time, all MD studies of glasses use quench rates which are several orders of magnitude higher than in experiments (the latter are typically 10^3 K s^{-1}). Despite this, MD studies have been able to provide key insights into the atomic structure of glasses, including SiO_2 glass (there is continuing investigation of the role of quench rates[30]). The fifth and sixth stages were temperature baths of 80 000 time steps each at 300 K (with and without equilibration, respectively). During the final stage the structural parameters were sampled every 200 time steps to represent the effects of disorder due to thermal vibrations, which is present in the experimental results. All of the results presented were obtained at 300 K.

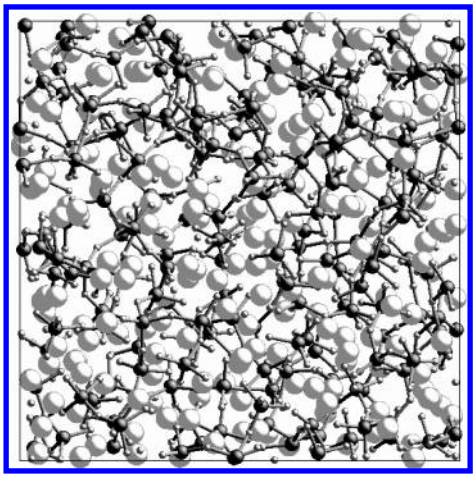

Figure 1. Image of $CaSiO_3$ glass model ($x = 0.5$) with spheres representing Ca, Si, and O (in decreasing order of radius), and sticks representing Si−O bonds.

3. Results

Figure 1 shows an image of the $CaSiO_3$ glass model ($x = 0.5$). Visual inspection indicates there is a tetrahedral silica network. Figure 2 shows the radial distribution functions $T_{ij}(r)$ for the $x = 0.5$ model, where

$$T_{ij}(r) = \frac{1}{r}\left(\frac{1}{N_i}\sum_{i=1}^{N_i}\sum_{j\neq i}^{N}\delta(r - R_{ij})\right) \qquad (2)$$

and $T_{ij}(r) \rightarrow 4\pi r\rho_j$ as $r \rightarrow \infty$ (where ρ_j is the atomic number density for element j). The first peak in $T_{SiO}(r)$ at ∼1.6 Å represents Si−O nearest neighbors. Oxygen atoms with 2 Si nearest neighbors have been classified as bridging oxygens, O_b, otherwise as nonbridging oxygens, O_{nb}. Table 4 shows the model has average $N_{SiO} = 4.03$ (a few 5-fold coordinated Si defects are present), and Figure 3 shows the O−Si−O bond angle is tetrahedral. The first peak in $T_{CaO}(r)$ at ∼2.4 Å represents Ca−O nearest neighbors (discussed below). $T_{OO}(r)$ has a first peak at ∼2.6 Å representing O coordinated to Si, i.e., O−Si−O configurations, and this is followed by a broad peak at ∼3.0 Å representing O coordinated to Ca, i.e., O−Ca−O configurations. $T_{SiSi}(r)$ has a first peak at ∼3.1 Å representing Si−Si neighbors in the silica network, which have a typical bond angle of ∼140° (see Figure 3). Si−Ca and Ca−Ca correlations overlap and are first prominent in the region 3.1−3.6 Å.

To describe the connectivity of the silica network, each Si is classified as Q^n, where n is the number of bridging oxygens, with the average denoted $\langle n\rangle$. As expected, for $x = 0$ (i.e., SiO_2) there is 100% Q^4 and $\langle n\rangle = 4$. As x increases there is a decrease in $\langle n\rangle$ (see N_{SiOb} in Table 4), and the distribution of Q^n becomes broad (see Figure 4). Note that $N_{SiO} = 4$ and $N_{SiOb} = \langle n\rangle$, so $N_{SiOnb} = 4 - \langle n\rangle$. The ratio of oxygen to Si is equal to $N_{SiOnb} + N_{SiOb}/2$ (since each O_b is shared between 2 Si), which equals $4 - \langle n\rangle/2$. This allows the value of $\langle n\rangle$ to be predicted from the

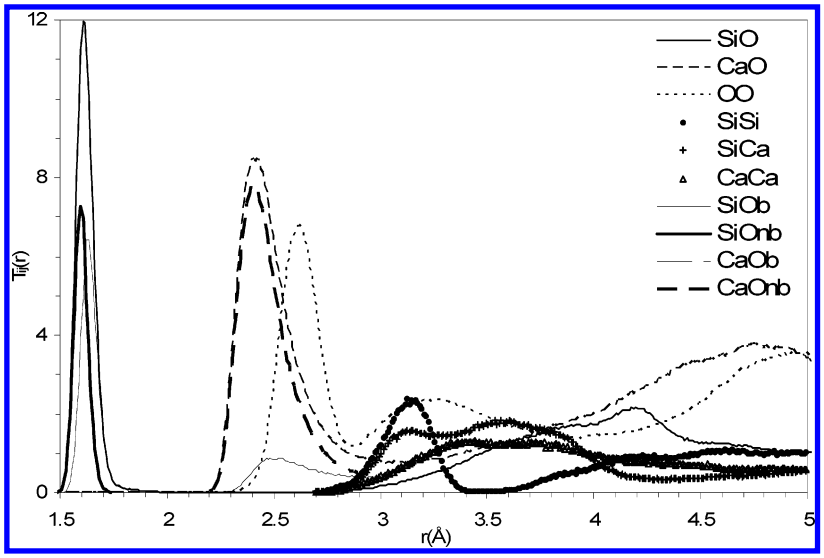

Figure 2. Radial distribution functions $T_{ij}(r)$ of a $CaSiO_3$ glass model ($x = 0.5$), including the distinction between bridging and nonbridging oxygens, i.e., O_b and O_{nb}, respectively. (Si−O correlations have been scaled $\times^1/_2$.)

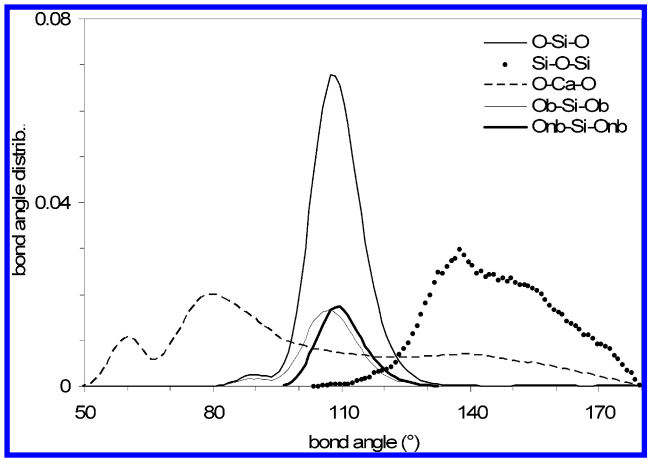

Figure 3. Bond angle distributions of a $CaSiO_3$ glass model ($x = 0.5$), including the distinction between bridging and nonbridging oxygens, i.e., O_b and O_{nb}, respectively. (O_b−Si−O_{nb} bond angles have been omitted for clarity.)

TABLE 4: Average Nearest Neighbor Distances, R_{ij}, and Coordination Numbers, N_{ij}, of $(CaO)_x(SiO_2)_{1-x}$ Glass Models

x	R_{SiO} (Å)	N_{SiO}	N_{SiOnb}	$N_{SiOb} = \langle n \rangle$	R_{CaO} (Å)	N_{CaO}	N_{CaOnb}	N_{CaOb}	N_{CaCa}
0	1.62	4.00	0.00	4.00					
0.1	1.62	4.00	0.22	3.78	2.37	5.4	3.1	2.3	1.8
0.2	1.62	4.00	0.50	3.51	2.40	5.4	3.7	1.7	2.8
0.3	1.62	4.01	0.85	3.15	2.41	5.9	4.4	1.5	4.2
0.4	1.61	4.02	1.31	2.71	2.42	6.3	5.0	1.3	5.8
0.5	1.61	4.03	1.94	2.09	2.41	6.4	5.4	1.0	7.0

composition, i.e., $(CaO)_x(SiO_2)_{1-x} \rightarrow Ca_{x/(1-x)}SiO_{(2-x)/(1-x)}$, hence the ratio of oxygen to Si is

$$4 - \frac{\langle n \rangle}{2} = \frac{2 - x}{1 - x} \qquad (3)$$

This gives values of $N_{SiOb} = \langle n \rangle = (4 - 6x)/(1 - x)$ which are in good agreement with values of N_{SiOb} shown in Table 4. The silica network contains rings of SiO_4 tetrahedra linked by O_b, and the distribution of ring sizes is shown in Figure 5 (note ring sizes >12 are not shown). As expected, there are much fewer rings and a much lower proportion of small rings for $x = 0.5$ compared to $x = 0$, due to the dominance of Q^2 units (see Figure 4). (These results show good correspondence with those for recent models of $(Na_2O)_x(SiO_2)_{1-x}$ glasses with x from 0 to 0.5.[15])

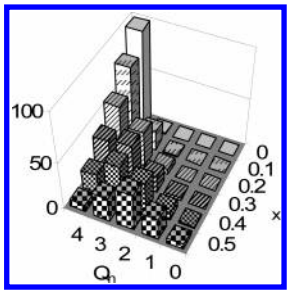

Figure 4. Connectivity of the silica network, i.e., distribution of Q^n, of $(CaO)_x(SiO_2)_{1-x}$ glass models.

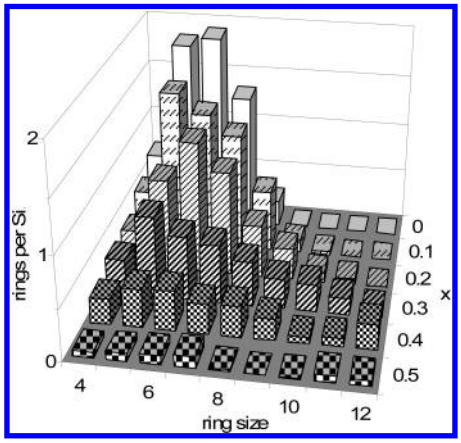

Figure 5. Distribution of ring sizes in the silica network of $(CaO)_x(SiO_2)_{1-x}$ glass models. (Note ring sizes >12 are not shown.)

The Ca−O coordination, N_{CaO}, was defined by using the minimum in $T_{CaO}(r)$ at 3.0 Å. Figure 6 shows the models have a narrow distribution of N_{CaO}. Table 4 shows the average of N_{CaO} is 6.3 in the glass-forming region, i.e., $x = 0.4$ and 0.5, and 5.4 in the phase-separated region, i.e., $x = 0.1$ and 0.2.The O−Ca−O bond angle for $x = 0.5$ (see Figure 3) represents CaO_N polyhedra, and is peaked at ~80° extending to 180° as expected for predominantly distorted octahedral coordination. A small peak at ~60° can be assigned to capped octahedra with $N_{CaO} = 7$. The values of N_{CaOnb} and N_{CaOb} are also shown in Table 4, and most of the Ca−O coordination is due to O_{nb}, as expected. However, there is a significant contribution from O_b,

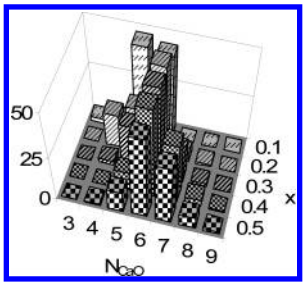

Figure 6. Distribution of Ca−O coordination numbers, i.e., N_{CaO}, of $(CaO)_x(SiO_2)_{1-x}$ glass models.

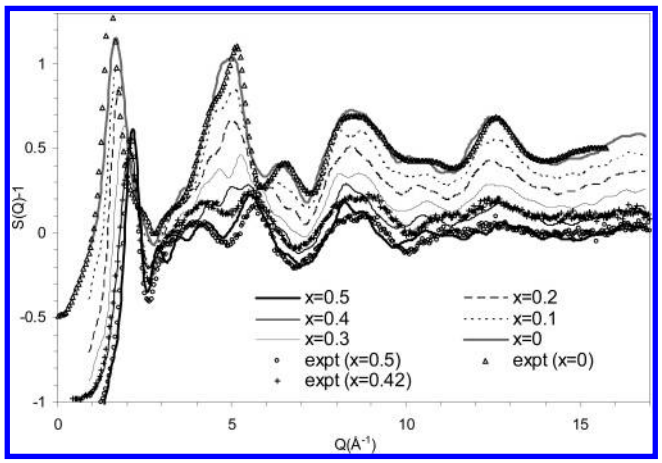

Figure 7. X-ray diffraction structure factors $S(Q)$ of $(CaO)_x(SiO_2)_{1-x}$ glass models, and from experiment for $x = 0$,[32] 0.42,[12] and 0.50.[12] (Vertical displacements of +0.1 have been used for clarity.)

with $N_{CaOnb} \sim 5$ and $N_{CaOb} \sim 1$ in the glass-forming region, changing to $N_{CaOnb} \sim 3$ and $N_{CaOb} \sim 2$ in the phase-separated region.

Changes in x have a predictable effect on $T_{ij}(r)$. As x decreases from 0.5 to 0, there is an increase in the heights of peaks at ~1.6, ~2.6, and ~3.1 Å due to Si−O nearest neighbors, O−Si−O configurations, and Si−Si neighbors (respectively). At the same time, there is a decrease in the heights of peaks at ~2.4, ~3.0, and 3.1−3.6 Å due to Ca−O nearest neighbors, O−Ca−O configurations, and Si−Ca/Ca−Ca correlations. The changes occurring in $T_{ij}(r)$ give changes in the diffraction structure factor $S(Q)$, where

$$Q(S(Q) - 1) = \sum_{ij} w_{ij}(Q) \int (T_{ij}(r) - r\rho_j) \sin(Qr)\, dr \quad (4)$$

and $w_{ij}(Q)$ is the weighting factor for scattering from correlations between elements i and j.[31] The values of $w_{ij}(Q)$ are different for X-rays and neutrons, and Figures 7 and 8 show the X-ray and neutron diffraction structure factors $S(Q)$ for the models.

The previous experimental studies for $CaSiO_3$ glass ($x = 0.5$) can be compared with the current model. The results for Ca coordination are reported in Table 5, and there is good agreement with the model. Experimental results for ^{29}Si NMR of $x = 0.5$ glass[10] gave a Q^n distribution of 19%, 55%, and 24% for Q^1, Q^2, and Q^3 (respectively), with uncertainty of a few percent. The model has a similar but somewhat broader Q^n distribution of 6%, 23%, 40%, 25%, and 8% for Q^0, Q^1, Q^2, Q^3, and Q^4 (respectively, see Figure 4). An ^{17}O NMR study of $x = 0.4$ glass was able to distinguish O_b and O_{nb}, but was not quantitative.[9] In a landmark experiment, double difference neutron diffraction with isotopic substitution was used to measure the Ca−Ca correlation in $CaSiO_3$ glass.[2] The results are shown in Figure 9, using the function $G_{CaCa}(r) = T_{CaCa}(r)$ $- 4\pi r\rho_{Ca}$, and the modeling results are in good agreement. This is of particular interest for theories of cation ordering in silicate glasses (see Discussion). Figures 7 and 8 also show limited experimental data for X-ray[12,32] and neutron[13,33] diffraction $S(Q)$ for glasses with $x = 0$,[32,33] 0.42,[12,13] and 0.5.[12] The modeling results are in reasonable agreement, and in particular reproduce well the behavior of the first sharp diffraction peak.

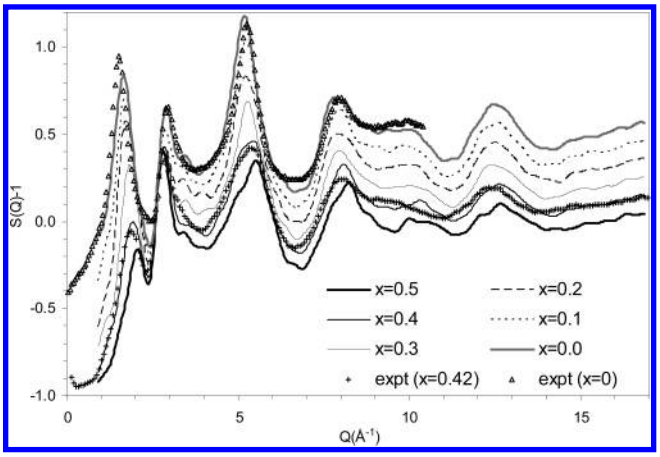

Figure 8. Neutron diffraction structure factors $S(Q)$ of $(CaO)_x(SiO_2)_{1-x}$ glass models, and from experiment for $x = 0$[33] and 0.42.[13] (Vertical displacements of +0.1 have been used for clarity.)

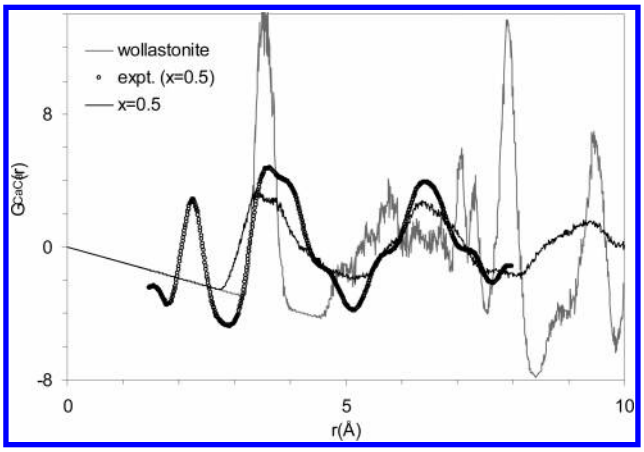

Figure 9. Ca−Ca correlation, in the form of $G_{CaCa}(r) = T_{CaCa}(r) - r\rho_{0Ca}$, for $x = 0.5$ from modeling, neutron diffraction,[2] and crystalline $CaSiO_3$ wollastonite. (The peak at 2.3 Å in neutron diffraction results was attributed to an artifact in the original study.[2])

TABLE 5: Comparison of Experimental and Modeling Results for Ca Coordination in $CaSiO_3$ Glass ($x = 0.5$)

method	R_{CaO} (Å)	N_{CaO}
X-ray diffraction[7]	2.44	
X-ray diffraction[8]	2.44 ± 0.01	
EXAFS[7]	2.49	5.6
EXAFS[8]	2.36 ± 0.01	6.0 ± 0.3
neutron diffraction[2]	2.37 ± 0.06	6.15 ± 0.17
current study	2.41 ± 0.02	6.4 ± 0.1

4. Discussion

As expected, the models in the glass-forming region, i.e., $x = 0.4$ and 0.5, have a corner-shared tetrahedral silica network, and Ca acts as a network modifier, preferring a coordination of 6 or 7.[34] The (distorted) CaO_N polyhedra are reminiscent of octahedra which are present in wollastonite $CaSiO_3$. Ca is predominantly coordinated to O_{nb}, but there is a significant contribution from O_b. For $x = 0.5$ there is $N_{CaOb} = 1.0$, and using $x_iN_{ij} = x_jN_{ji}$ gives $N_{ObCa} = 1.0$. Hence on average each

O_b is bonded to 2 Si plus 1 Ca. This is expected to weaken/lengthen $Si-O_b$ bonds, and strengthen/shorten $Si-O_{nb}$ bonds in compensation, and this is seen in the $T_{SiO}(r)$ (see Figure 1) and O−Si−O bond angle distribution (see Figure 2). This is also consistent with an ^{17}O NMR study of $x = 0.4$ glass, which found a noticeable interaction between O_b and Ca.[9] There are strong similarities with the short-range order in crystalline $CaSiO_3$ wollastonite, in which Ca has a mixture of 6- and 7-fold coordination, each O_b is coordinated to 2 Si and 1 Ca, and there is lengthening of $Si-O_b$ bonds and shortening of $Si-O_{nb}$ bonds.

The similar role of O_b in the $CaSiO_3$ glass model and in wollastonite may be a consequence of geometric constraints on the sharing of O_{nb} among Ca (i.e., arranging several Ca around one O_{nb}). Using $x_i N_{ij} = x_j N_{ji}$ with $x_{Onb} = x_{Si} N_{SiOnb}$, $N_{SiOnb} = 4 - \langle n \rangle$ and eq 3 shows $N_{OnbCa} = N_{CaOnb}/2$ for all x. If Ca was not coordinated to O_b, i.e., $N_{CaOb} = 0$, then the observed value of $N_{CaO} = 6.4$ for $x = 0.5$ would require $N_{CaOnb} = 6.4$ and $N_{OnbCa} = 3.2$, so on average each O_{nb} would be bonded to 1 Si plus 3 or 4 Ca. This may be geometrically difficult to arrange. In contrast, the observed values of $N_{CaOb} = 1.0$ and $N_{CaOnb} = 5.4$ require $N_{OnbCa} = 2.7$, so on average each O_{nb} is bonded to 1 Si plus 2 or 3 Ca. (Recent modeling of $(Na_2O)_x(SiO_2)_{1-x}$ glass with $x = 0.5$[15] has shown a similar role of O_b with $N_{NaOb} = 0.8$ and $N_{NaOnb} = 4.3$.)

The Ca−Ca correlation in $CaSiO_3$ glass ($x = 0.5$) was previously measured by using double difference neutron diffraction with isotopic substitution.[2] The Ca−Ca correlation in the form of $G_{CaCa}(r)$ was interpreted as being similar to that in wollastonite, where edge-sharing CaO_6 octahedra are arranged in sheets. This interpretation was based on the first and second peaks in the Ca−Ca distribution being approximately in the ratio $1:\sqrt{3}$, which is expected for two-dimensional close-packing of CaO_N polyhedra.[2] Figure 9 shows that the experimental results for $G_{CaCa}(r)$ are not similar to those for wollastonite, but are similar to those for the $x = 0.5$ model, and Figure 1 shows that the $x = 0.5$ model does not contain Ca arranged in sheets. Hence the results of the present study do not substantiate the previous theory of modifier cation ordering.

Although the focus of the present study is on the glass-forming region, i.e., $x = 0.4$ and 0.5, the results may also provide insight into phase separation, expected for $x = 0.1$ and 0.2 (with $x = 0.3$ being intermediate). The characteristics of the silica network, as shown by Q^n and ring size distributions, appear to follow a smooth trend as x decreases from $x = 0.5$ to 0 (see Figures 4 and 5). However, there is a noticeable difference in short range order around Ca. For $x = 0.1$ and 0.2 (compared to $x = 0.4$ and 0.5) there are lower values of $N_{CaO} = 5.4$ (compared to $N_{CaO} = 6.3$), and higher values of $N_{CaOb} \sim 2$ (compared to $N_{CaOb} \sim 1$). The former means $N_{CaO} < 6$, and the latter means on average each CaO_N polyhedra is edge sharing with ~2 SiO_4 tetrahedra, hence the short range order around Ca in the phase-separated region is energetically less favorable.

Phase separation in the $CaO-SiO_2$ liquid involves the coexistence of Ca-poor and Ca-rich liquids, hence the glasses with $x = 0.1$ and 0.2 are expected to contain Ca-rich regions. Ca clustering has been investigated by calculating N_{CaCa}, the average number of neighboring Ca around a given Ca (defined by using a cutoff of 5.0 Å corresponding to the minimum in $T_{CaCa}(r)$). The values of N_{CaCa} are shown in Table 4 and appear to follow a smooth trend, decreasing from $N_{CaCa} = 7.0$ for $x = 0.5$ to $N_{CaCa} = 1.8$ for $x = 0.1$. They can be compared with estimates for a homogeneous distribution of Ca, where the number of Ca in a spherical volume of radius 5 Å would be $4\pi/3 \times (5\ \text{Å})^3 \times \rho_{Ca}$, which equals 7.9 for $x = 0.5$ and 1.2 for $x = 0.1$. However, since one Ca is the central Ca and the rest are neighboring Ca, this gives estimates of $N_{CaCa} = 6.9$ for $x = 0.5$ and $N_{CaCa} = 0.2$ for $x = 0.1$. This suggests that for $x = 0.1$ the Ca are clustered rather than homogeneously distributed (and similarly for $x = 0.2$). Clustering is also indicated by the value of $N_{CaOnb} = 3.08$ for $x = 0.1$, which corresponds to $N_{OnbCa} = 1.5$, so on average half of O_{nb} are bonded to 1 Si plus 2 Ca.

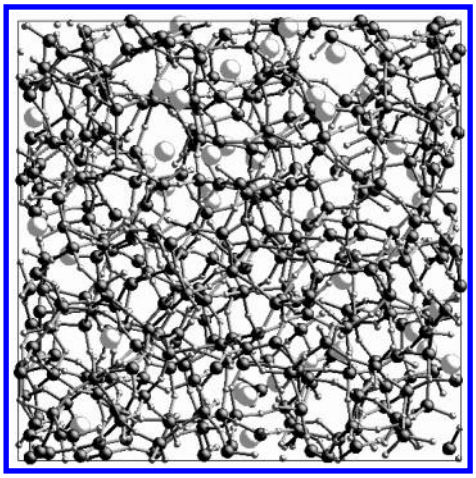

Figure 10. Image of the $x = 0.1$ model with spheres representing Ca, Si, and O (in decreasing order of radius), and sticks representing Si−O bonds. The upper part of the model contains a large Ca cluster, i.e., Ca-rich region, whereas the central part of the model contains no Ca, i.e., a Ca-poor region.

TABLE 6: Distribution of Ca Cluster Sizes of $(CaO)_x(SiO_2)_{1-x}$ Glass Models (where Ca that share a common O are defined to belong to the same cluster)

x	no. of Ca in model	no. of Ca in cluster (× no. of clusters)				
0.5	200	200				
0.4	160	160				
0.3	120	120				
0.2	80	69	4 (×2)	1 (×3)		
0.1	40	13	10	3	2 (×3)	1 (×8)

Individual clusters of Ca in the models were identified by defining 2 Ca which are bonded to a common O to belong to the same cluster. The connections between adjacent CaO_N polyhedra within clusters was investigated by calculating the average number of oxygens which are shared between 2 neighboring Ca. Average values of ~1.6 were obtained for all x (values of 1, 2, and 3 correspond to corner, edge, and face-sharing, respectively). However, there is a dramatic change in cluster sizes with x, as shown in Table 6. For $x = 0.3$, 0.4, and 0.5 (see Figure 1) all Ca are part of single clusters which span the models, i.e., Ca is fully distributed within the silica network. In contrast, for $x = 0.2$ and 0.1 there are one or two clusters of Ca much larger than expected for a homogeneous distribution (see Table 6). Figure 10 of the $x = 0.1$ model shows a large Ca cluster in the upper part, i.e., a Ca-rich region, and a central part with just two isolated Ca, i.e., a Ca-poor region. The low proportion of isolated Ca is understandable, since isolated Ca require O_{nb} bonded to just 1 Si plus 1 Ca, and this is energetically unfavorable considering the typical bond valences of ~1 for Si−O bonds and ~$^1/_3$ for Ca−O bonds.

5. Conclusions

Models of $(CaO)_x(SiO_2)_{1-x}$ glasses contain a tetrahedral silica network, the connectivity of which decreases as x increases. In the glass-forming region, i.e., $x = 0.4$ and 0.5, Ca has a mixture of 6- and 7-fold coordination. An important role is played by bridging oxygen, each of which is on average coordinated to 2

Si plus 1 Ca. This short range order is similar to that in wollastonite. The $x = 0.5$ model is in satisfactory agreement with previous experimental studies of $CaSiO_3$ glass. In particular, it is in good agreement with a key neutron diffraction measurement of the Ca−Ca correlation, and does not substantiate the previous theory of modifier cation ordering that predicted Ca is arranged in sheets. In the phase-separated region, i.e., $x = 0.1$ and 0.2, there is marked clustering of Ca, and this can be understood as a preference to avoid having O_{nb} bonded to just 1 Si and 1 Ca.

Acknowledgment. We are grateful to EPSRC for funding, to A. N. Cormack and J. Du for advice about molecular dynamics modeling, and to anonymous referees for helpful criticisms.

References and Notes

(1) Kerner, R.; Phillips, J. C. *Solid State Commun.* **2001**, *117*, 47.
(2) Eckersley, M. C.; Gaskell, P. H.; Barnes, A. C.; Chieux, P. *Nature* **1988**, *335*, 525. Gaskell, P. H.; Eckersley, M. C.; Barnes, A. C.; Chieux, P. *Nature* **1991**, *350*, 675.
(3) Martinez, A.; Izquierdo-Barba, I.; Vallet-Regi, M. *Chem. Mater.* **2000**, *12*, 3080. Saravanapavan, P.; Hench, L. L. *J. Non-Cryst. Solids* **2003**, *318*, 1.
(4) Hudon, P.; Baker, D. R. *J. Non-Cryst. Solids* **2002**, *303*, 299.
(5) Doweidar, H. *J. Non-Cryst. Solids* **1999**, *249*, 194.
(6) Matsuraba, E.; Kawazoe, R.; Waseda, Y.; Ashizuka, A.; Ishida, E. *J. Mater. Sci.* **1988**, *23*, 547.
(7) Taniguchi, T.; Okuno, M.; Matsumoto, T. *J. Non-Cryst. Solids* **1997**, *211*, 56.
(8) Mastelaro, V. R.; Zanotto, E. D.; Lequeux, N.; Cortes, R. *J. Non-Cryst Solids* **2000**, *262*, 191.
(9) Lee, S. K.; Stebbins, J. F. *J. Phys. Chem. B* **2003**, *107*, 3141.
(10) Zhang, P.; Grandinetti, P. J.; Stebbins, J. F. *J. Phys. Chem. B* **1997**, *101*, 4004.
(11) Ohashi, Y. *Phys. Chem. Mineral.* **1984**, *10*, 217.
(12) Mountjoy, G. *SRS Experimental Reports 2005*; Daresbury Laboratory: Warrington, 2005; RB42218.
(13) Karlsson, C.; Zanghellini, E.; Swenson, J.; Roling, B.; Bowron, D. T.; Borjesson, L. *Phys. Rev. B* **2005**, *72*, 064206.
(14) Abramo, M. C.; Caccamo, C.; Pizzimenti, G. *J. Chem. Phys.* **1992**, *96*, 9083.
(15) Cormack, A. N.; Du, J. *J. Non-Cryst. Solids* **2001**, *293*−*295*, 283.
(16) Belashchenko, D. K.; Ostrovski, O. I.; Skvortsov, L. V. *Thermochim. Acta* **2001**, *372*, 153.
(17) Delaye, J. M.; Cormier; Ghaleb, D. L.; Calas, G. *J. Non-Cryst. Solids* **2001**, *293*−*295*, 290.
(18) Matsui, M. *Phys. Chem. Miner.* **1996**, *23*, 345.
(19) Gale, J. D. *J. Chem. Soc., Faraday Trans.* **1997**, *93*, 629. Version 1.2. 2002.
(20) Natta, G.; Passerini, L. *Gazz. Chim. Ital.* **1929**, *59*, 129.
(21) Norby, P. *J. Appl. Crystallogr.* **1997**, *30*, 21.
(22) Czaya, R. *Acta Crystallogr. B* **1982**, *24*, 1968.
(23) Yang, H. X.; Prewitt, C. T. *Am. Mineral.* **1999**, *84*, 929.
(24) Fletcher, D. A.; McMeeking, R. F.; Parkin, D. *J. Chem. Inf. Comput. Sci.* **1996**, *36*, 746.
(25) Smith, W.; Forester, T. *J. Mol. Graphics* **1996**, *14*, 136.
(26) Sen, S.; Andrus, R. L.; Baker, D. E.; Murtagh, M. T. *Phys. Rev. Lett.* **2004**, *93*, 125902.
(27) Webb, S. L. *Am. Mineral.* **1991**, *76*, 1449.
(28) Doremus, R. H. *Glass Science*; John Wiley and Sons: New York, 1973; **1**p 105.
(29) Forsbacka, S.; Holappa, L. *Scand. J. Metall.* **2004**, *33*, 261.
(30) Corrales, L. R.; Du, J. *Phys. Chem. Glasses* **2005**, *46*, 420.
(31) Elliott, S. R. *Physics of Amorphous Materials*; Longman: Harlow, 1990; p 91.
(32) Bionducci, M.; Buffa, F.; Licheri, G.; Musinu, A.; Navarra, G.; Piccaluga, G. *J. Non-Cryst. Solids* **1994**, *177*, 137.
(33) Wicks, J. D.; McGreevy, R. L.; Borjesson, L. *Phase Trans.* **1997**, *61*, 195.
(34) Chiari, G. *Acta Crystallogr. B* **1990**, *46*, 717.